Photoelectrochemistry of Si/Polymer and Si/Metal/Solution Interfaces

Thesis by

Christoph D. Karp

Submitted In Partial Fulfillment of the Requirements
for the Degree of Master of Science

Division of Chemistry and Chemical Engineering
California Institute of Technology
Pasadena, California

1995

(submitted November 16, 1994)

Acknowledgements

First of all, I would like to thank Nate Lewis, my advisor at Caltech. I think I may have been one of the most stubbornly resistive people in regards to doing some of the things that were expected of me, and I'm sure that at times it was not easy to have me as a student. However, Nate managed to teach me a lot about semiconductors, and also the methodology of science in general. I would also like to thank Ken Goldsby and Spence Slattery from FSU, for influencing my decision to dive into the swimming pool of science.

I have been privileged to work with some excellent people at Caltech. Mike Freund, Paul Laibinis, Ming Tan, and Randy Lee have all spent countless hours teaching me about science; they each made the work enjoyable for me. Rich Muller and Paul Maker at JPL were both very helpful, and did great work with the e-beam lithography. Also, thanks to Siamak Forouhar at JPL, who was always available if I had any problems or questions.

Thanks also to the other members of the Lewis Group, who were helpful in many different discussions, and always kept a steady supply of pens for me on their desks: Chris Kenyon, Chris Claypool, Chris Wilisch, Gary Shreve, Ashish Bansal, Janet Kesselman, Teri Longin, Kathy Pomykal, Arnel Fajardo, Sonbinh Nguyen, Iver Lauermann, Marcel Sturzenegger, and Bruce Tufts.

Thanks to Pat Anderson, who struggled valiantly to keep the Lewis Group from missing all of its deadlines. Pam Schaeffer has done a great job of

following a hard act to follow. Also, thanks to Dian Buchness for running the Chemistry Department so well.

So much for science. One of the best things about Caltech is the quality of the people I have met here. Bob Blake, chef extraordinaire and pinball wizard; Tim Herzog, who coached the soccer team and also planned a most excellent camping trip; Nancy, Gary and Ben Shreve; Chris and Cathy and Emily and Karla Wilisch; the Lewis and Bercaw groups; the Chemistry Soccer Team. Thanks to all of you for making Maria and I feel very much at home in Southern California.

Above all, I would like to thank my beautiful wife Maria. She is truly an exceptional person, and no man can hope to ever receive more love and support than she has given to me.

Abstract

Part I of this thesis describes the formation of a silicon/polypyrrole junction utilizing a new method of polypyrrole polymerization which was developed in the Lewis Group by Dr. Michael Freund. This new method involves the chemical oxidation of pyrrole to form smooth, conducting polypyrrole films upon solvent evaporation. This polymerization process allows semiconductor/polymer junctions to be formed without exposing the silicon surface to harmful oxidative currents used in electrochemical polymerizations. The studies described herein demonstrate the formation of a stable, rectifying junction between silicon and chemically polymerized polypyrrole.

Part II of this thesis describes work related to a recent hypothesis regarding the charge-transfer processes of metal-coated silicon electrodes in methanol solutions, proposed by Ming Tan of the Lewis Group. The silicon is modified by depositing thin metal lines onto the surface, which facilitate electron-transfer between the silicon and the solution and limit direct charge transfer through the silicon/solution interface. The design of these devices allows examination of the interaction of semiconductor/metal and semiconductor/liquid junction characteristics as a function of the size and distribution of metal lines.

TABLE OF CONTENTS

Acknowledgements	ii
Abstract	iii
Table of Contents	iv
List of Figures	vi
Part I: Characterization of Silicon/Polypyrrole Junctions	1
Abstract	2
Introduction	3
Experimental	6
Results and Discussion	8
Conclusion	14
References	15
Part II: Studies of Charge Transfer Processes in Silicon/Metal/$Me_2Fc^{+/0}$-Methanol Junctions	17
Abstract	18
Introduction	19
Experimental	23
Results and Discussion	
Part 1: Device Fabrication	27

Part 2: I-V Characteristics of Silicon/Gold Junctions 32

Part 3: Modification of Electrode Design 43

Part 4: I-V Characteristics of Silicon/Platinum Junctions 48

Conclusion 53

References 54

LIST OF FIGURES

Part I

Figure 1. SEM of polypyrrole film 9

Figure 2. Cyclic voltammogram of polypyrrole film 10

Figure 3. I-V curve of silicon/polypyrrole junction 12

Part II

Figure 1. Schematic of theory for silicon/metal-line/solution electrical junctions 21

Figure 2. Illustration of photolithography procedure 26

Figure 3. SEM of incomplete metal liftoff 30

Figure 4. SEM of 100 nm wide gold lines 31

Figure 5. Plot of ln I vs. V_{oc} for silicon electrodes patterned with 5 mm-wide metal lines in $Me_2Fc^{+/0}$-methanol solution 34

Figure 6. Plot of ln I vs. V_{oc} for silicon electrodes patterned with 5 mm-wide and 100 nm-wide metal lines in $Me_2Fc^{+/0}$-methanol solution 35

Figure 7. Same as figure 6, except the current has been normalized to the metal area 38

Figure 8. Plot illustrating the deterioration of I-V properties of silicon electrodes patterned with 100 nm-wide gold lines in $Me_2Fc^{+/0}$- methanol solution 39

Figure 9. SEM of silicon electrode with detached gold lines 42

Figure 10. Schematic of new electrode design 45

Figure 11. SEM of crossbar contacting 5 μm-wide platinum lines 47

Figure 12. I-V properties of silicon electrodes patterned with 5 μm-wide platinum lines, in $Me_2Fc^{+/0}$-methanol solution and in air 49

Figure 13. I-V properties of silicon electrodes patterned with 0.34 μm-wide platinum lines, in $Me_2Fc^{+/0}$-methanol solution and in air 50

Part I

Characterization of Silicon/Polypyrrole Junctions

Abstract

We have investigated the properties of the electrical junction formed between n-type silicon and chemically polymerized polypyrrole. Earlier studies have shown that polypyrrole forms electrical junctions with silicon. These junctions were found to have current-voltage characteristics that were independent of the electrochemical potential of the polypyrrole, which is not the case for some other studies involving interfaces between silicon and conducting polymers. These previous silicon/polypyrrole interfacial studies, however, were performed on junctions fabricated using electrochemical growth of the polypyrrole onto the silicon. This process exposes the silicon surface to harmful oxidative current during the polymer growth step, and can lead to oxidative passivation of the silicon. This would affect the interpretation of current-voltage measurements, because the insulating oxide layer would add an additional resistance to the junction formed between silicon and polypyrrole. By chemically depositing the polymer from a solution, we have minimized the possibility of oxidation of the silicon surface. We have explored the possibility that the chemical deposition of polypyrrole onto silicon forms junctions with different electrical properties than those formed by the electrochemical growth of polypyrrole onto silicon. A comparison of results from these two different methods of polymer deposition may offer added insight into the nature of silicon/conducting polymer interfaces.

Introduction

Silicon/Conducting Polymer Junctions

Using conducting polymers that have different electrochemical potentials can create large differences in the current-voltage properties of the silicon/polymer interface, as has been shown for junctions between silicon and reduced vs. oxidized polyacetylene[1,2]. In examining the junction formed between a semiconductor and a metal, varying the electrochemical potential of the metal phase requires variation in the metal. It has been observed that the junction properties of the different silicon/metal junctions are not dependent on the work-functions of the metals[3,4]. This phenomenon, known as Fermi-level pinning, has been rationalized as being due to the formation of surface states between the metal and silicon. The electrical characteristics of the silicon/metal junction are dependent on the interface between the semiconductor and the surface states, and changing the contacting metal will thus have little effect on the current-voltage characteristics of such systems. Conducting polymers have therefore been shown to have potential advantages over metals in forming electrical junctions with silicon.

Not all studies of junctions formed between silicon and conducting polymers have shown ideal behavior. Experiments using electrochemically grown polypyrrole on silicon electrodes seem to indicate that changing the redox potential of the polypyrrole does not have as much of an effect on the current-voltage properties as would be expected[5,6]. Growing polypyrrole electrochemically onto silicon, however, results in the passage of harmful oxidative currents through the silicon, which may corrode, passivate, or otherwise change the surface. Thus, using a process that does not form surface states during the formation of a junction between silicon and polypyrrole may be important in obtaining the desired response of current-

voltage characteristics to changes in the electrochemical potential of the polymer.

Soluble Conducting Polymers

Substantial effort has been directed at producing stable, processible conducting polymers in order to fabricate uniform, well-defined polymer structures[7]. The most rigorously pursued strategy for making soluble, and therefore processible, conducting polymers has been to attach bulky side chains to the polymer backbone. This prevents the efficient packing of polymer chains and increases solubility. Although this strategy has been successful, there is a tradeoff between solubility and conductivity. This results from the fact that twisting of the polymer backbone decreases the conjugation length in the polymer. An approach which has been utilized successfully to increase the conjugation length in the polymer backbone while maintaining solubility has been polymerization of monosubtituted cyclooctatetraenes to form substituted polyacetylenes[1,2]. However, even under optimal conditions, the conductivity of such systems is over an order of magnitude less than in nonsubstitued polyacetylene.

An alternative route to producing processible conducting polymers is to utilize polymerization reactions in which monomer coupling is the rate determining step in the overall polymerization reaction. Under these conditions polymerization will be concentration dependent, and can therefore be controlled by manipulating the solution conditions. For example, dilute, relatively unreactive solutions containing monomer, polymerization agent, and dopant can be prepared and deposited onto substrates, where polymerization occurs as the solvent evaporates and the solution becomes more concentrated.

In this work we have investigated the chemical polymerization of pyrrole. This reaction belongs to the family of polymerization reactions in which oxidation of monomer is followed by radical cation coupling, and in which the coupling reaction is the rate determining step[9-11]. A common characteristic of these reactions is that the oxidation potentials of the monomers are significantly higher than those of the oligomers[9]. As a result, polymerization becomes thermodynamically more favorable as it proceeds. One example of this is the polymerization of pyrrole using $FeCl_3$ as the oxidant[12-15]. However, we have found that using $FeCl_3$ causes the rapid precipitation of polymer from solution. Our system utilizes phosphomolybdic acid (PMA) as the oxidant and dopant source. PMA has an oxidizing potential that does not cause rapid polymerization of pyrrole in solution. We thus have been able to produce solutions containing pyrrole monomer and oxidant which remain stable for periods of several hours. Polymerization to produce thin, well defined films is achieved by coating a substrate and allowing the solvent to evaporate. This procedure does not produce soluble polymer films, but allows the deposition of a conducting polymer in a controlled manner.

Experimental

Materials

Pyrrole and phosphomolybdic acid were obtained from Aldrich and were used as received. Tetrahydrofuran, acetonitrile, methanol (Omnisolv grade) and KCl were obtained from EM Science, and tetrabutylammonium perchlorate (TBAP) was obtained from Sigma. Tetrahydrofuran was distilled over Na/benzophenone and acetonitrile was distilled over CaH_2 and then over P_2O_5; methanol was distilled over Mg. Substrates for optical and conductivity measurements were either Pyrex glass slides or Indium Tin Oxide (ITO) coated glass slides. Si (1 ohm-cm resistivity) was obtained from Silicon Sense (Nashua, NH). Electrodes were fabricated by scratching the back of the silicon with a diamond scribe, applying In/Ga eutectic to this roughened surface and then connecting a tinned copper wire using silver print. The back and sides of this electrode were then encased in non-conducting epoxy.

Measurements

Optical spectra were obtained on a Hewlett Packard 8452A spectrophotometer, interfaced to an IBM XT. Electrochemical experiments were performed with a Princeton Applied Research 173 potentiostat/175 universal programmer. All electrochemical experiments were performed with a Pt flag auxiliary and a saturated calomel reference electrode (SCE). Spin coating was performed on a Headway Research photoresist spin coater. Film thickness was determined with a Sloan Dektak 3030 profilometer. Conductivity measurements were performed with an Alessi Instruments osmium-tipped four point probe (tip spacing - 0.050", tip radii - 0.010"). Light for photovoltage and photocurrent measurements was supplied using an ELH bulb and various neutral density filters to adjust the light intensity.

Film Polymerization

N_2-purged solutions of pyrrole (1.50 mmoles in 4 ml tetrahydrofuran) and phosphomolybdic acid (0.75 mmoles in 4 ml tetrahydrofuran) were injected into a N_2 purged test tube. The mixture immediately became dark green, with no observable precipitation over the next several hours. This solution was used for film preparation within an hour of mixing, and was filtered through a Gelman 0.1 μm pore size teflon filter immediately before use. Polymerization occured after depositing the mixture described above on a substrate (e.g. glass, Si, filter paper, etc.) and allowing the solvent to evaporate. Polymerization was indicated during this process by a change in film color from green to black. Once polymerization was completed, the film was insoluble and was rinsed with solvent (tetrahydrofuran or methanol) to remove residual reduced phosphomolybdic acid and unreacted monomer. The thin films of polypyrrole used for optical and scanning electron microscopy (SEM) measurements were produced by spin-coating the solution described above onto a glass or ITO/glass substrate at ~2000 RPM. This procedure resulted in uniform film thickness of 40-100 nm, depending on spin velocity.

Results

Physical Properties of Chemically Oxidized Polypyrrole

Conductivities of methanol-rinsed polypyrrole films on glass slides, as determined by four point probe measurements, were on the order of 15-30 S cm^{-1}. These values are typical for an unoptimized synthesis. These conductivities were stable in air over several days. The blue film that was initially formed, which contained reduced phosphomolybdic acid, had a very low conductivity that was difficult to determine experimentally. However, after rinsing the film, the conductivity increased markedly. Rinsing these films in methanol also allowed the film to be lifted from the surface of the glass. The ability of our films to be removed from the substrate and remain intact argues against the possibility that they could just be deposits of powdered polymer. In addition, SEM of these films showed that they had a smooth morphology and were defect free at high magnification (Figure 1).

This morphology contrasted with the rough, globular structures and large pores of films that are obtained by electrochemical deposition of polypyrrole[8-10]. Elemental analysis of the rinsed films revealed a relatively high concentration of phosphorous, molybdenum and oxygen. However, it is difficult at this time to determine the stoichiometry of the film and which species are present as counterions, compared to those that are merely trapped in the polymer.

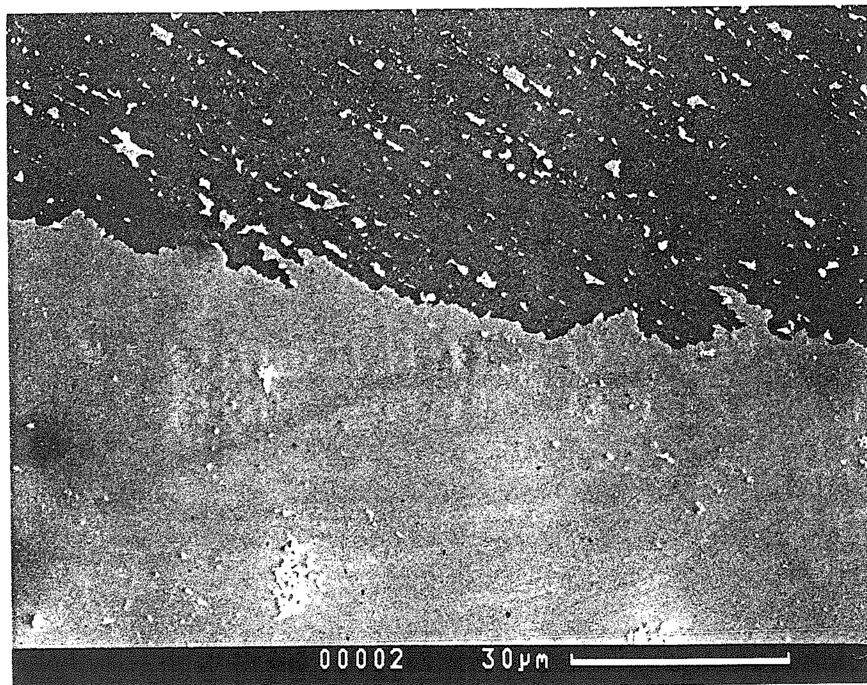

Figure 1. SEM of polypyrrole film formed by the chemical polymerization of pyrrole using phosphomolybdic acid. The film has been scraped from the substrate in the top of the picture.

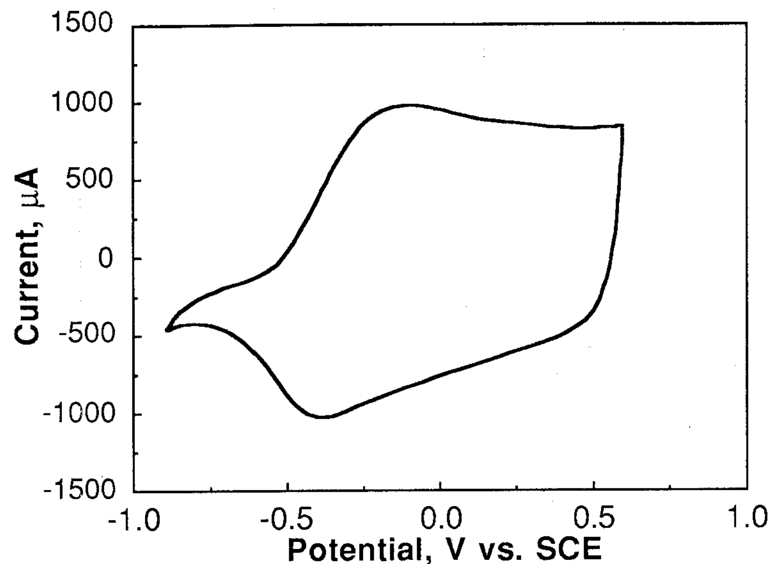

Figure 2

The polypyrrole films exhibited excellent electrochemical properties. In order to study the electrochemical properties of the polypyrrole films, Pt electrodes were dipped into pyrrole/phosphomolybdic acid solutions. The electrodes were then allowed to dry, leaving them with a thin film of polypyrrole. After rinsing the films in methanol and allowing them to dry in air, cyclic voltammograms were obtained in 0.1 M TBAP/acetonitrile. Figure 2 shows the redox behavior of a chemically polymerized polypyrrole film following ten cycles from -1.0 V to +0.7 V (versus SCE). The cathodic wave at -0.4 V corresponds to the reduction of polypyrrole to its neutral, non conducting state. The anodic wave at -0.2 V corresponds to the reoxidation of polypyrrole to its conducting state. The lack of additional faradaic current which would result from the oxidation and reduction of phosphomolybdic acid suggests that the keggin structure of phosphomolybdic acid is not retained. This is contrary to what has been observed with polypyrrole which

has been polymerized electrochemically in the presence of phosphotungstic acid[16,17].

I-V properties of Si/polypyrrole junction

Our method of producing polypyrrole allows junctions to be formed with Si which have rectifying properties, and show excellent current-voltage characteristics (figure 3). At short-circuit photocurrent densities (J_{ph}) of 20 mA/cm^2, open-circuit photovoltage (V_{oc}) values are 0.53V, compared to 0.58V for the same type of Si in a methanol solution of Dimethylferrocene$^{+/0}$. The chemically oxidized polypyrrole reported here protects against Si corrosion in aqueous solutions over time periods comparable to electrochemically grown polypyrrole on Si[18]; however, long term stabilities have not yet been achieved.

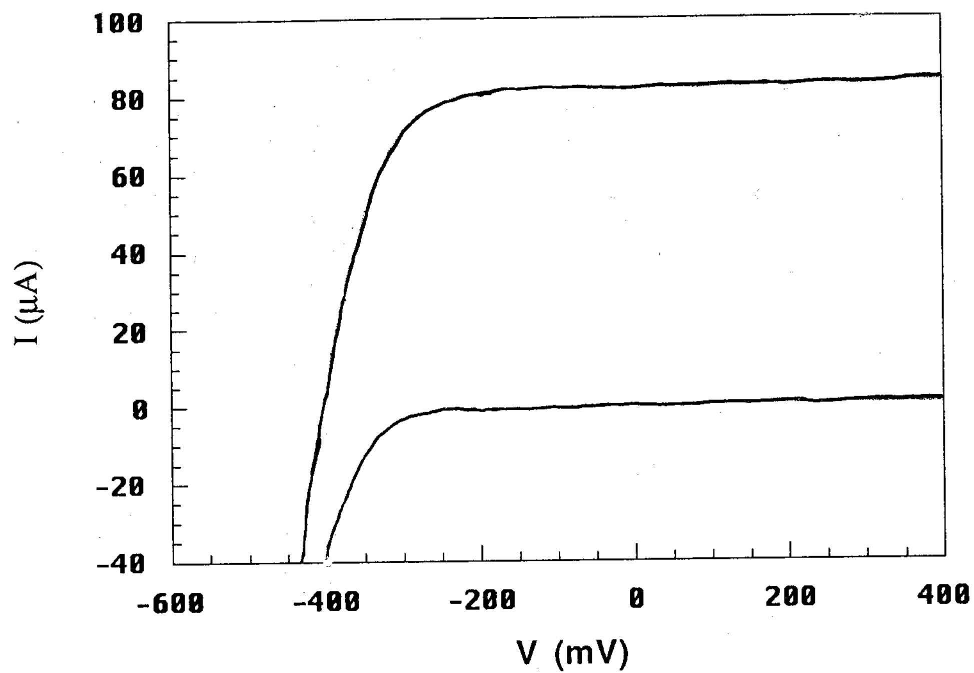

Figure 3. Current-voltage curve for a junction formed between n-silicon and chemically polymerized polypyrrole. The lower curve is data taken in the dark; the upper curve is data taken in the light.

Discussion

Pyrrole polymerization

The mechanism of pyrrole polymerization begins with cation radical formation upon oxidation of pyrrole. This is followed by a cation radical coupling mechanism to form dimers[19,20]. Dimers, which are more easily oxidized than monomers, go on to form radical cations which will further couple with monomer or dimer radical cations. Because the j-mers are increasingly more easily oxidized as j increases, the process is expected to continue. The film that is formed is conductive because it remains in the oxidized state at the completion of polymerization.

Based on this mechanism, one would predict a cascading effect upon polymerization initiation. Under conditions where a chemical oxidant (Ox) is introduced to a solution of pyrrole (Py), where $E_{pyrrole} > E_{Ox}$, there will besome finite, *albeit* small, concentration of oxidized pyrrole monomer ($Py^{\cdot +}$) as predicted by the Nernst equation. Since pyrrole oxidation is fast, as $Py^{\cdot +}$ is consumed by the radical coupling reaction, it will be maintained at the initial equilibrium concentration governed by the Nernst equation. As solvent evaporation occurs and the solution becomes more concentrated, the ratio of $[Py^{\cdot +}]/[Py]$ will remain constant. However, the concentration of $[Py^{\cdot +}]$ will increase and so will the rate of the coupling reaction. Since the coupling reaction is the rate determining step, the rate of polymerization will be expected to increase during solvent evaporation.

Phosphomolybdic acid is a relatively strong oxidant ($E^\circ = +0.36$ V), although it is not a sufficiently strong oxidizing agent to significantly oxidize pyrrole monomer ($E^\circ = +1.3$ V)[7]. The difference in formal potentials predicts that the oxidation of pyrrole monomer by phosphomolybdic acid is unfavorable. It has been shown that the oxidation potential of pyrrole

oligomers decreases from +1.2 V to +0.55 to +0.26 V as the number of units increases from one to two to three, and that the oxidation potential of bulk polypyrrole occurs at -0.1 V[11]. As a result, oxidation of the oligomers by phosphomolybdic acid will become thermodynamically favorable.

Conclusion

We have successfully determined a method to produce polypyrrole films via chemical oxidation of pyrrole, and have utilized this method to produce a rectifying junction with silicon. Further experiments will be aimed at determining if the manipulation of the redox potential of polypyrrole on silicon will cause the ideal current-voltage behavior. We have used a literature synthesis to prepare (3-pyrrole)acetic acid[21,22], which can be polymerized to form conductive films that have a pH-dependent electrochemical potential. We plan to electrochemically polymerize this polymer onto the surface of silicon, and to compare these junctions with the analogous junctions formed using the chemical oxidation of pyrrole. By changing the pH of the solution, we will be able to adjust the electrochemical potential of the polymer over several hundred millivolts. This will allow us to determine if the current-voltage characteristics of the silicon/poly(3-pyrrole)acetic acid junctions are dependent on the electrochemical potential of the polymer for each method of polymer deposition. This may lead to further insight into the mechanism of charge-transfer between silicon and conducting polymers.

References

(1) Sailor, M.J.; Klavetter, F.L.; Grubbs, R.H.; Lewis, N.S. *Nature*, **1990**, *346*, 155-157.

(2) Sailor, M.J.; Ginsburg, E.J.; Borman, C.B.; Kumar, A.; Grubbs, R.H.; Lewis, N.S. *Science*, **1990**, *249*, 1146-1149.

(3) Sze, S.M. *Physics of Semiconductor Devices*, 2nd ed.; J. Wiley: New York, 1981.

(4) Tan, M.X.; Laibinis, P.E.; Nguyen, S.T.; Kesselman, J.M; Stanton, C.E.; Lewis, N.S. *Progress in Inorganic Chemistry*, **1994**, *41*.

(5) Holdcroft, S.; Funt, B. *J. Electrochem. Soc.* **1988**, *135*, 3106-3109.

(6) Skotheim, T.; Petersson. L.-G.; Inganas, O.; Lundstrom, I. *J. Electrochem. Soc.* **1982**, *129*, 1737-1741.

(7) Skotheim, T.A. (Ed.), *Handbook of Conducting Polymers*, Marcel Dekker: New York, 1986, vol. 1 and 2.

(8) Zinger, B.; Shaier, P.; Zemel, A. *Synth. Met.* **1991**; *40*, 283-297.

(9) Ko, J.M.; Rhee, H.W.; Park, S.-M.; Kim, C.Y. *J. Electrochem. Soc.* **1990**, *137*, 905-909.

(10) Pei, Q.; Qian, R. *Synth. Met.* **1991**, *45*, 35-48.

(11) Diaz, A.F.; Crowley, J.; Bargon, J.; Gardini, G.P.; Torrance, J.B. *J. Electroanal. Chem.* **1981**, *121*, 355-361.

(12) Kaeriyama, K.; Masuda, H. *Synth. Met.* **1991**, *41*, 389-392.

(13) Kaeriyama, K.; Masuda, H. *Synth. Met.* **1991**, *41*, 393-396.

(14) Whang, Y.E.; Han J.H.; Motobe, T.; Watanabe, T.; Miyata, S. *Synth. Met.* **1991**, *45*, 151-161.

(15) Machida, S.; Miyata, S. *Synth. Met.* **1989**, *31*, 311-318.

(16) Bidan, G.; Genies, E.M.; Lapkowski, M. *J. Electroanal. Chem.* **1988**, *251*, 297-306.

(17) Lapkowski, M.; Bidan, G.; Fournier, M. *Synth. Met.* **1991**, *41-43*, 407-410.

(18) Noufi, R.; Frank, A.J.; Nozik, A.J. *J. Am. Chem. Soc.* **1981**, *103*, 1849-1850.

(19) Andrieux, C.P.; Audebert, P.; Hapiot, P.; Savéant, J.-M. *J. Am. Chem. Soc.* **1990**, *112*, 2439-2440.

(20) Andrieux, C.P.; Audebert, P.; Hapiot, P.; Savéant, J.-M. *J. Phys. Chem.* **1991**, *95*, 10158-10164.

(21) Delabouglise, D. *Synth. Met.*, **1992**, *51*, 321-327.

(22) Delabouglise, D.; Garnier, F. *New J. Chem.* **1991**, *15*, 233-234.

Part II.

Studies of Charge Transfer Processes in

Silicon/Metal/$Me_2Fc^{+/0}$-Methanol Junctions

Abstract

Using standard photolithographic methods, we have deposited arrays of metal lines onto silicon to fabricate unique electrodes. The current-voltage properties of these electrodes in methanol solutions of dimethylferrocene have been investigated. Part I describes the investigations of the charge-transfer mechanisms of systems that simultaneously attained the high efficiency of a silicon/solution junction and possessed the stability of a silicon/metal junction. Several different versions of these modified electrodes have been examined to determine the effects of changing both the dimensions of the metal lines and the extent of the metal coverage.

It appeared that decreasing the width of gold lines deposited on silicon, while maintaining a constant silicon/gold junction area, caused a large increase in the efficiency of the metal-coated silicon electrode in solution. Contrary to this result, a decrease in the dimensions of platinum lines deposited on silicon electrodes caused a decrease in the efficiency of these electrodes in solution, compared to electrodes with wider platinum lines and identical platinum coverage areas. The mechanism behind this behavior is still not understood.

Introduction

Semiconductor/metal junction devices have been extensively studied as systems for the conversion of solar energy into electrical energy[1-3]. However, these systems typically exhibit much lower efficiency than is theoretically possible. Conversely, semiconductor/liquid junctions have been shown to be highly efficient at solar energy conversion[2], but chemical reactions often occur between the semiconductor surface and the solution to corrode or passivate the semiconductor, thus limiting the potential usefulness of these systems. The use of a thin metal overlayer on the surface of the semiconductor produces devices that are immune to passivation and oxidation processes, and are therefore stable in solution. However, this metal layer prevents the direct interaction between the semiconductor and solution, thus again limiting the efficiency of the system.

Studies by Nakato and others[5-9] have shown that a discontinuous film of metal deposited on the surface of silicon can protect the silicon from passivation in aqueous electrochemical cells. These studies are intriguing because the metal film apparently gives protection against oxidation of the semiconductor while simultaneously allowing manipulation of the semiconductor Fermi-level through the chemical composition of the solution, thus providing high efficiency cells. The analysis of the charge-transfer measurements made in these experiments are somewhat ambiguous. The area of metal/silicon contact relative to the area of solution/silicon contact is not known with accuracy, so it is difficult to determine the

contribution of the different interactions between semiconductor, metal and solution. In addition, there may be corrosion processes taking place at the bare silicon surface, which would interfere with current-voltage measurements.

In order to better understand these semiconductor/metal/solution hybrid systems, we have undertaken a more systematic study where metal lines of known width are deposited onto silicon using photolithographic techniques. This will allow us to know the exact areas of the semiconductor that are in contact with metal or exposed to solution. By varying the width of the lines and the spacing between them, a wide range of hybrid junctions can be formed with different metal/solution contact ratios, thus allowing the prediction and verification of the current-voltage properties of the devices. Our studies use solution electrochemical systems based on outer-sphere redox couples in methanol, which are stable and well characterized[1,2]. This limits the possibility of any corrosion process of the silicon interfering with the measurements. By doing this experiment, we hope to gain insight into the mechanisms of charge-transfer at metal-coated semiconductors in solutions. This could lead to the development of high efficiency, small band-gap semiconductor electrodes which will be stable in aqueous electrochemical cells.

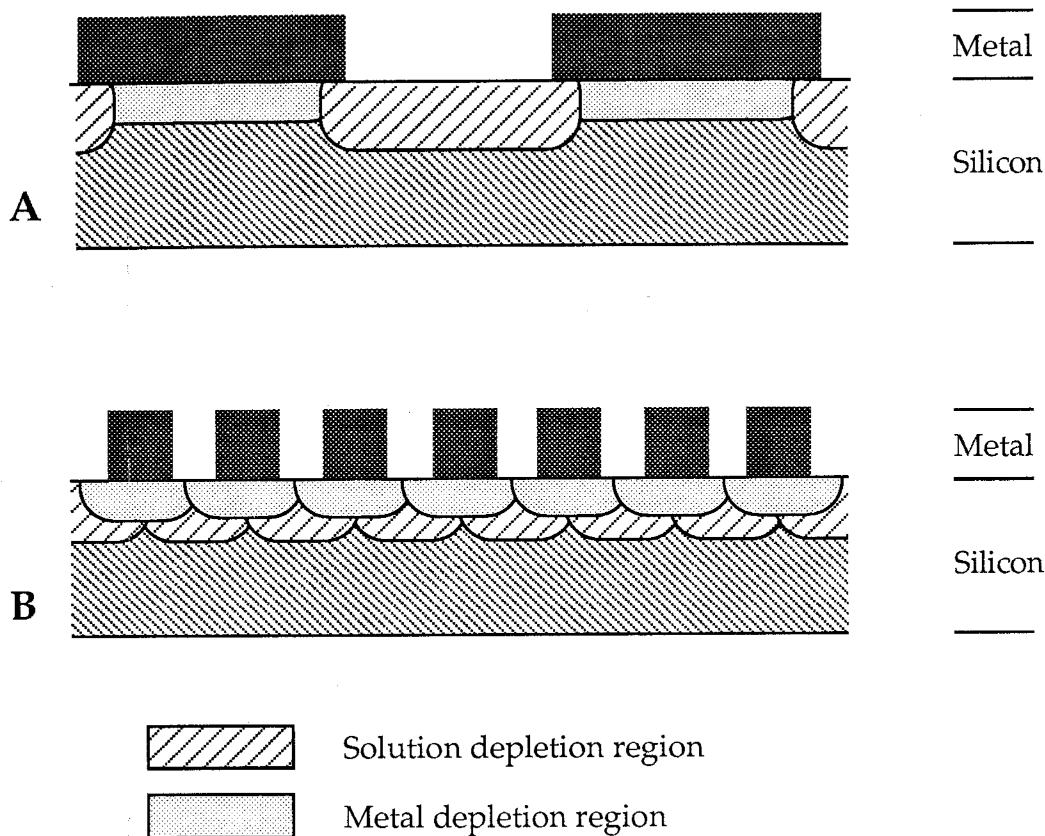

Figure 1 Schematic illustrating the two situations for electrodes in this study. A) Shows the discrete depletion regions formed underneath large-width metal and solution contacts to the semiconductor. B) Shows the possible overlap of depletion regions when the contacts are narrowed in width; in this diagram, the solution depletion region has been drawn shielding the metal depletion region from the semiconductor.

Figure 1 is an illustration of the two basic parts of the theory[4] that this study has examined. Metal/silicon and solution/silicon contact areas having large widths (figure 1A) form two different and separate types of depletion regions in the semiconductor. In this system, the shallower depletion region formed by the silicon/metal junction will dominate the overall characteristics of the charge transfer process, because current can flow through this interface more easily. However, as the width of the metal/silicon contact areas are made very narrow (less than the solution depletion width), the silicon/solution depletion regions will essentially overlap beneath the metal contacts and shield the silicon/metal interface (Figure 1B) from the interior of the semiconductor. Thus, the effects of the silicon/metal junction on the overall charge-transfer process for majority carriers will be reduced; an electron approaching the interface from the interior of the silicon will no longer have available the lower energy pathway leading to the surface of the silicon through the depletion region formed by the silicon/metal interface. Thus, I_0, the saturation recombination current, of this system will be much lower than expected, resulting in higher efficiency. At the same time, the metal deposited on the surface will facilitate minority carrier transfer to the solution, thus avoiding the oxidation of the silicon[1-3].

Experimental

Photolithography and SEM characterization were done in collaboration with Dr. Paul Laibinis, in the clean-room of the Microdevice Laboratory at the NASA Jet Propulsion Laboratory (JPL). Electrode fabrication and solution electrochemical characterization was done in collaboration with Ming Tan, at the California Institute of Technology.

47 Ω-cm resistivity n-Si, (100) orientation, was obtained from Silicon Sense (Nashua, NH). Buffered HF solution was obtained from Transene Corp. Methanol, Omnisolv grade, was obtained from EM Science and distilled over Mg. Me_2Fc was obtained from Aldrich and purified by sublimation. Photolithographic masks used to fabricate the 5 μm line-width patterns were obtained from Micro Mask, Inc. The sub-1 μm line-width patterns were drawn directly onto the silicon surface by Rich Muller and Paul Maker at JPL using electron-beam lithography.

Current-voltage measurements were made using a Princeton Applied Research 173 potentiostat/175 universal programmer. $Me_2Fc^{+/0}$-methanol electrochemical cells were operated under a nitrogen atmosphere, with a Pt wire counter electrode referenced against the cell potential. Illumination from an ELH bulb was used to determine the photovoltage and photocurrent; the intensity of this light was varied by using neutral density filters. A constant stream of air was directed at the front of the cell and a 10 cm path-length water filter was placed between the light source and the cell to prevent increases in temperature of the cell due to the heat from the light source.

Electrode Fabrication

The Si wafers were first cleaned in a Branson/IPC oxygen plasma asher (which essentially forms an atmosphere of oxygen radicals) for 5 minutes at 50 watts in 0.5 torr O_2, to remove residual organic films from the surface. The oxide layer formed on the silicon surface during the oxygen plasma ashing process was subsequently removed by etching in 10% HF solution for 2 minutes. Figure 2 shows the image-reversal fabrication process used for the deposition of the 5 μm wide metal lines. The clean silicon wafers were first spin-coated with AZ5214-E photoresist (Figure 2A) on a Headway Research spin-coater at 4500RPM for 40 seconds, and then baked at 95^0 C for 2 minutes. The coated wafer and the mask were then placed in a Karl Suss MJB3 mask aligner and exposed to UV light for 45 seconds. After hard-baking the photoresist-coated silicon wafer at 120^0C for 2 minutes, the wafer was completely exposed (without the mask) to the UV light for 2x45 seconds. The photoresist was then developed in AZ 400K developer (20% by volume in water) for 30 seconds to remove the exposed areas of the photoresist (Figure 2B). The patterned wafers were then cleaned in the oxygen plasma for 30 seconds and etched for 1 minute in 10% HF, to remove any residual photoresist and oxide from the exposed silicon area on which metal was to be deposited. The patterned wafers were placed into a Sloan SL1800 e-beam evaporator within 10 minutes of the final HF etch to ensure minimal growth of oxide on the surface. The pressure in the evaporator was allowed to reach $<10^{-6}$ torr. Gold (or platinum) was then deposited at a thickness of ca. 600 Å

(Figure 2C). A liftoff in acetone removed the residual photoresist and left the desired metal line pattern (Figure 2D). The wafer was then diced into individual squares (8 mm x 8 mm) using a Micro Automation Inc. Model 1006 diamond saw.

Electrical contacts to these squares were made by roughening the back surface with a diamond scribe and gently scratching In/Ga eutectic into this area. The squares were then made into electrodes by connecting a wire to this back contact using silver print, and encasing the back and edges of the silicon in insulating epoxy so that only the front surface was exposed to solution. Care was taken to avoid covering with epoxy any part of the metal line pattern on the front surface of the silicon.

The sub-1 μm line-width electrodes were made in a similar fashion, except for the process used to create the pattern of lines in the photoresist. The sub-1 μm wide lines were individually drawn directly onto photoresist-coated silicon using electron-beam lithography; all of the other fabrication procedures were the same as those followed to make the 5 μm line-width electrodes.

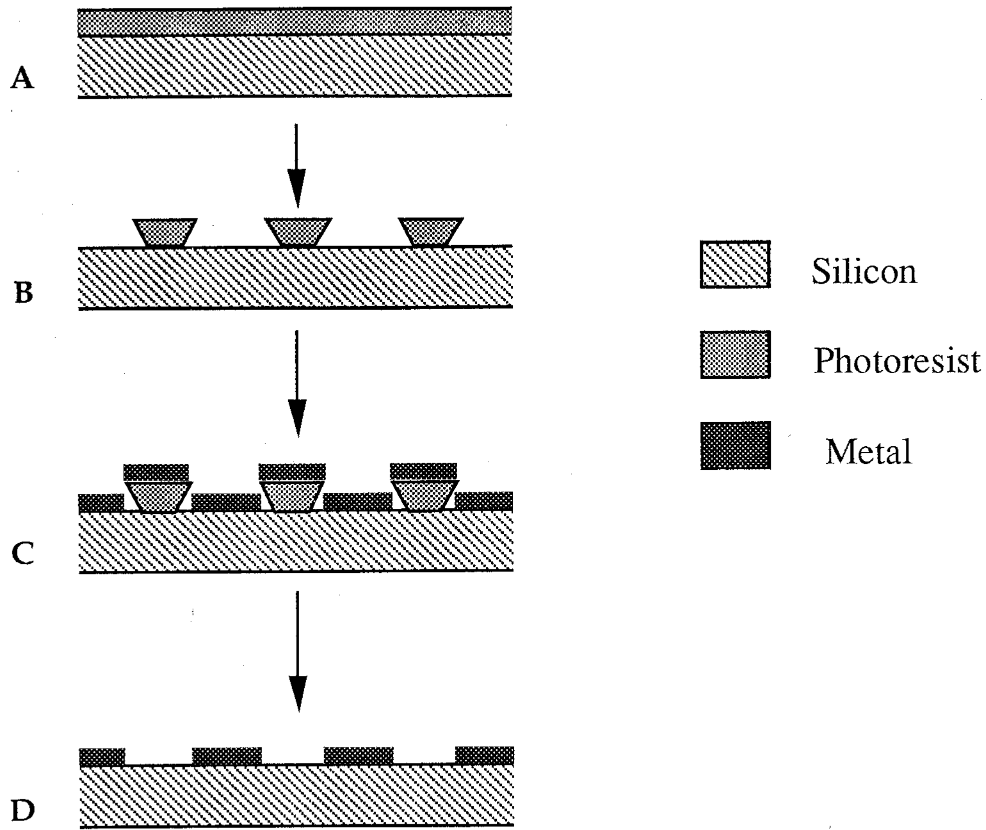

Figure 2: Schematic of the process used to fabricate the metal-line patterns on the silicon surface. A) Photoresist is spin-coated onto cleaned silicon wafer; B) Line pattern is made by exposure of UV light through a mask, using image-reversal process; C) Metal film is evaporated onto surface in vacuum; D) Photoresist is dissolved in acetone, removing unwanted metal. The negatively-sloping walls of the photoresist in C) allow unwanted metal to be easily removed from surface.

Results and Discussion

Part 1: Device Fabrication

The positive-type photoresist used in the fabrication of the 5 μm line-width patterns undergoes a photo-induced chemical reaction when exposed to UV light[10]. Part of the polymer undergoes a rearrangement to form a carboxylic acid side chain; the side chain allows this exposed area of the polymer to be soluble in basic aqueous solutions while the unexposed areas remain insoluble. In contrast, the image-reversal process involves several added steps which cause the reverse situation to occur, where the initially exposed area remains insoluble, and the masked area becomes soluble in basic aqueous solutions. After the initial UV exposure, for image-reversal the photoresist is heated to drive off the carboxylic acid side chain as CO_2. A flood exposure then creates carboxylic acid side chains in the rest of the polymer, which can then be dissolved in aqueous base. Thus, the pattern of exposed silicon is an exact image of the portion of the mask that blocks UV light.

The image-reversal process is important in the fabrication of these types of structures, because the negative-sloping sidewalls of the resist that this process creates (Fig 2C) greatly reduce the possibility of an incomplete lift-off. The SEM of an incomplete liftoff is shown in figure 3. In some areas of this pattern, metal could not be removed from between the patterned lines. This probably resulted from an improperly done image-reversal, which allowed the metal to form an unbroken layer covering both the exposed silicon and the photoresist. Properly developed photoresist using the image-

reversal process has sidewalls that slope in such a manner as to cause the metal to be deposited in discrete layers, preventing unwanted metal from being anchored to the silicon.

The electron-beam lithography process works in a fundamentally different manner than conventional photolithography, but produces essentially the same results[11]. The electron beam is focused to a narrow spot which is moved over the substrate in the desired pattern. Where the beam strikes the photoresist it breaks up the molecules of the polymer, and subsequent development removes the exposed area. This process is for practical purposes limited to a minimum of ~100 nm feature size. This limit is a consequence of several factors. The spot size of the electon-beam, which is adjusted by increasing or decreasing the current in the electron-beam, has a minimum size of approximately 30 nm. Thus, features with dimensions of ~30 nm could conceivably be drawn. However, decreasing the current causes the rate of exposure of the photoresist to also decrease, and this increases the time required to draw a line of a given length. The 4 mm^2 pattern of 100 nm lines separated by 400 nm (figure 4) required approximately 80 hours of electron-beam time[12]. Increasing the time required to draw a pattern will also increase the likelihood of drift (where the beam wanders from the programmed pattern) and current spikes (which produce large, undesired areas of exposed photoresist, essentially "holes" in the pattern).

In general, our devices did not experience many problems with poor adhesion that is typically found when depositing gold or platinum directly on

silicon. The oxygen plasma ashing and final HF etch done after photoresist development and immediately before metal deposition remove any traces of photoresist and silicon oxides from the developed areas of the pattern and create a clean silicon surface for metal deposition. Another factor that was probably involved in the good metal/silicon adhesion of our devices is the lack of airborne particles in the clean-room air. There are approximately 10^6 times more particles in a given volume of normal Los Angeles air than in clean-room air; these particles can adhere to the silicon surface and interfere with adhesion of the deposited metal to the silicon. Metals deposited in the clean-room on silicon had excellent adhesion lasting months after deposition, and could not be peeled off by Scotch Tape (a common testing procedure).

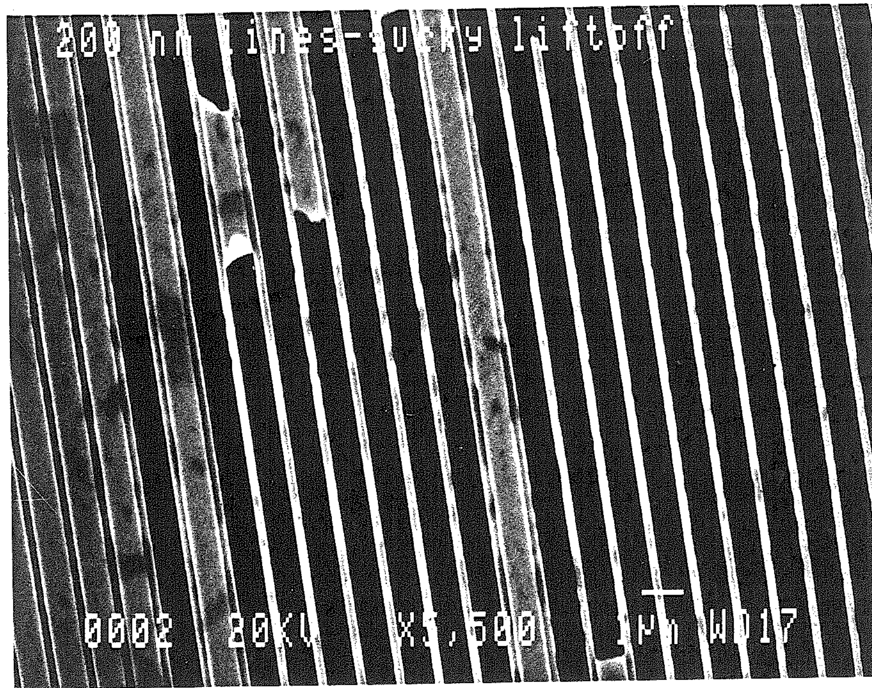

Figure 3: SEM of incomplete liftoff. The bright narrow lines are the desired metal pattern. Between several of the metal lines, areas of metal that should have been removed during the liftoff procedure remain firmly attached.

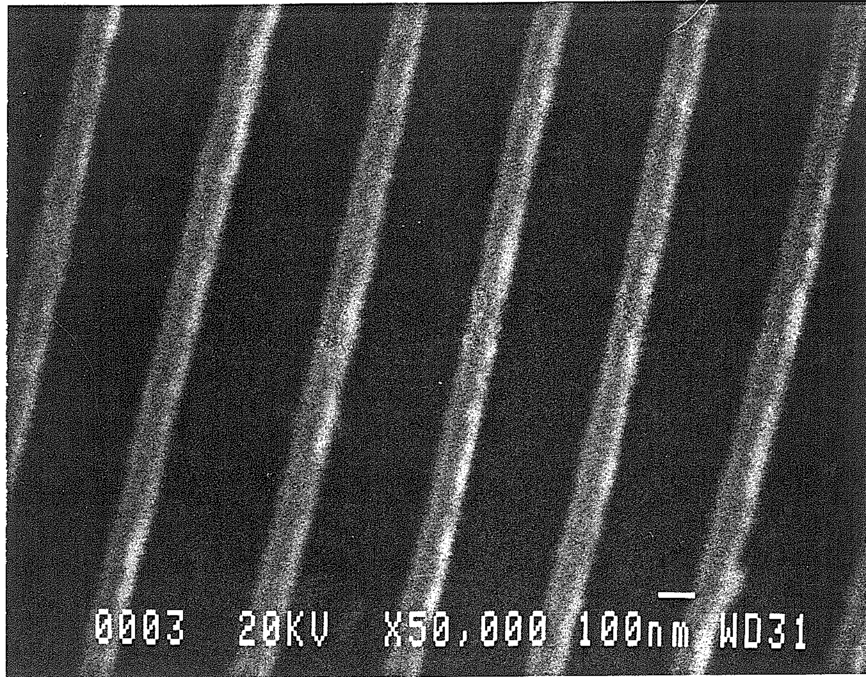

Figure 4: SEM of deposited metal lines having a width of ~100 nm.

Part 2: I-V Characteristics of Silicon/Gold Junctions

Figure 5 shows a plot of the current-voltage data under illumination of silicon electrodes patterned with 5 μm-wide metal lines in $Me_2Fc^{+/0}$-methanol solution, as a function of total metal coverage. Plotting the log of the photocurrent against the photovoltage yields a straight line with a y-intercept equal to I_0. I_0 essentially represents current that is not flowing in the required direction through the cell; as the value of I_0 increases, the efficiency of the electrode decreases[1,3]. The data for each metal coverage ratio was reproducible within 5% for at least five different electrodes.

Tan's treatment states that at metal line-widths much larger than the solution-induced depletion region in the silicon, these devices will merely exhibit area-weighted averages of silicon/solution and silicon/metal I-V properties[4]. As predicted, a shift in photovoltage was seen for the electrodes with 5μm wide lines as the coverage of metal was varied; a larger ratio of bare silicon to metal covered silicon (and thus smaller absolute amount of metal) produced a larger photovoltage at a given photocurrent. The increasing silicon/solution junction area relative to the silicon/metal junction area resulted in a larger average depletion width in the silicon. This resulted in a more efficient separation of photogenerated charge carriers, and thus a higher photovoltage. Alternatively, one can picture a decrease in the average I_0 as a larger percentage of the silicon is exposed to the solution; V_{oc} increases logarithmically as I_0 decreases[1]. It should be noted, however, that even for an electrode with only a 1% metal coverage the current-voltage characteristics

are significantly different from those of a bare Si electrode in the same solution, i.e. the metal is still "evident".

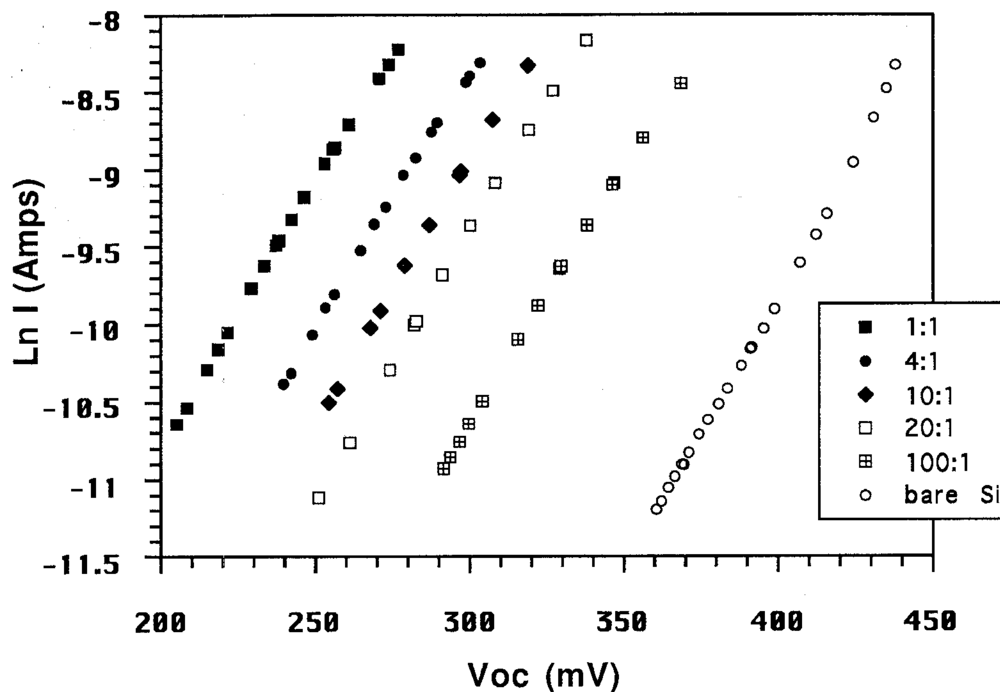

Figure 5: Plot of ln (photocurrent) vs. photovoltage for silicon electrodes patterned with 5 μm-wide metal lines in $Me_2Fc^{+/0}$-methanol solution, as a function of total metal coverage. The different points for each data set are taken at various light intensities. The legend indicates the ratio of the area of exposed silicon to the area of metal covered silicon.

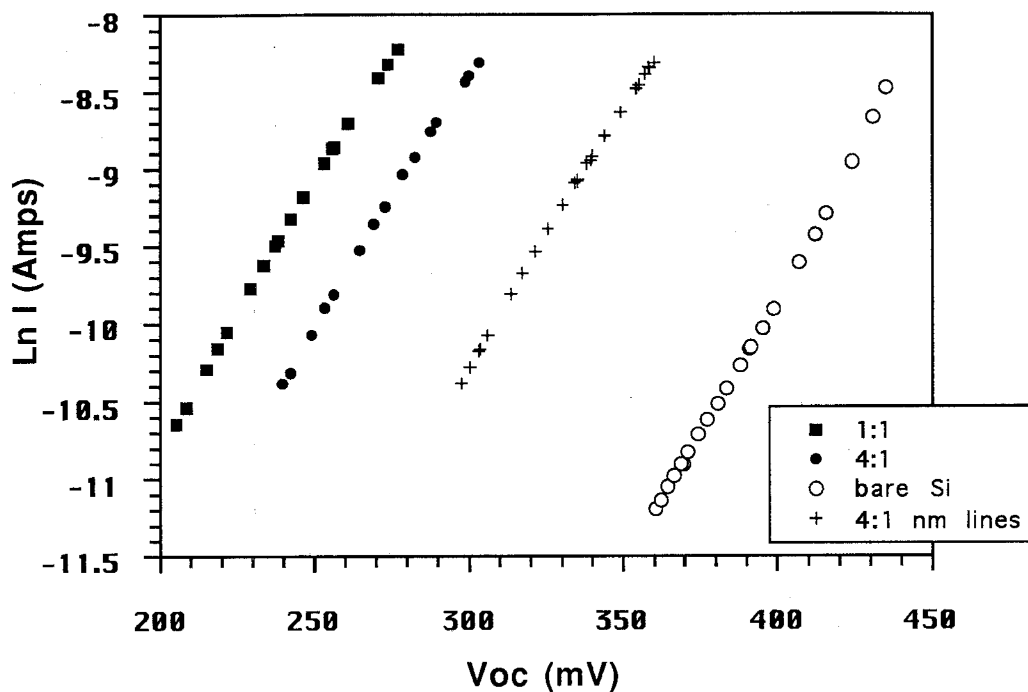

Figure 6: Plot of ln (photocurrent) vs. photovoltage at various light intensities for silicon electrodes patterned with 5 μm-wide metal lines in $Me_2Fc^{+/0}$-methanol solution, as a function of total metal coverage. The legend indicates the ratio of the area of exposed silicon to the area of metal covered silicon. In addition, data for a silicon electrode patterned with 200 nm-wide metal lines has been incorporated into this plot. Note the difference between this electrode and the electrode patterned with 5 μm-wide metal lines at the same metal coverage ratio (4:1).

Figure 6 shows selected data from figure 5, but also includes the data from an electrode with 100 nm-wide gold lines for comparison. The current-voltage properties of this electrode are very different from those of the electrode with equal area of metal coverage with 5 μm-wide gold lines. For a given voltage the current obtained from the electrode with the 100 nm-wide gold lines is much less than would be expected based on the amount of metal contacting the silicon. This can be explained by assuming that the solution depletion region is extending underneath the metal contacts and partially shielding the metal depletion region; this results in an effective decreased area of metal as seen by the electrode. However, the solution contacts do not in this case fully overlap to completely shield the silicon from the metal depletion regions, as the current-voltage characteristics would then be identical to the bare Si electrode in solution.

Another way to examine this data is by plotting the photocurrent divided by the metal area of the electrode vs. the open circuit photovoltage. This plot (figure 7) uses the assumption that the photocurrent of the electrode was due mainly to the silicon/metal interface. This is a good assumption for the electrodes that had a higher percentage of metal coverage because the I_0 for the metal/silicon junction was ~2-3 orders of magnitude greater than that of the solution/silicon junction, so it is reasonable to expect that most of the charge-transfer occured through the silicon/metal junction. By plotting this data for electrodes with two different ratios of metal coverage, it is more evident that the metal contact dominated the I-V properties; if there were a

significant amount of charge-transfer through the silicon/solution junction, then the different areas of solution/silicon contact for each electrode would give different "current density" values when normalized to the metal area. As can be seen in figure 7, the data for two electrodes with 5 μm-wide metal lines but with different metal areas line up together when plotted this way. Thus the photocurrent per metal area was constant for electrodes with 5 μm-wide metal lines. However, the electrode with 100 nm-wide lines lies somewhere between the electrodes with the 5 μm-wide metal lines and the bare silicon electrode in its I-V properties. This indicates that the electrode with 100 nm-wide lines had a lower current than the electrodes with the 5 μm-wide metal lines, at the same area of metal coverage. Thus, the silicon/gold junction formed in the electrode with 100 nm-wide lines can be considered to have a smaller effective junction area than was expected based on the geometrical area of the gold pattern.

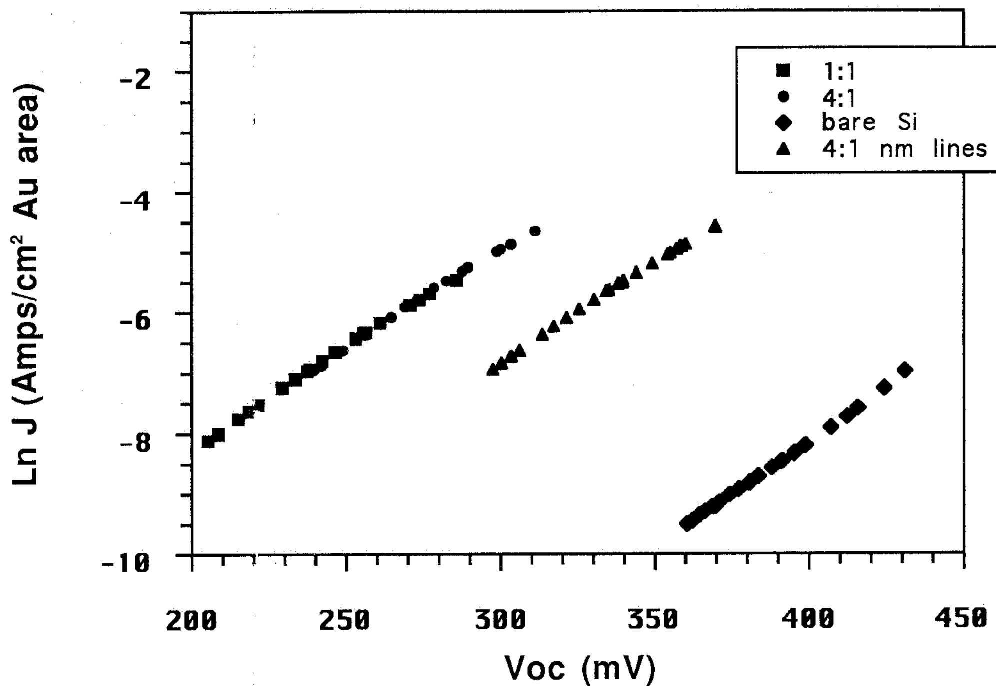

Figure 7 Plot of ln (photocurrent/Au coated area) vs. photovoltage for silicon electrodes patterned with 5 μm-wide metal lines in $Me_2Fc^{+/0}$-methanol solution, as a function of total metal coverage. The legend indicates the ratio of the area of exposed silicon to the area of metal covered silicon. The electrode patterned with 100 nm-wide gold lines had a smaller photocurrent density than would be expected based on the total area of metal coverage.

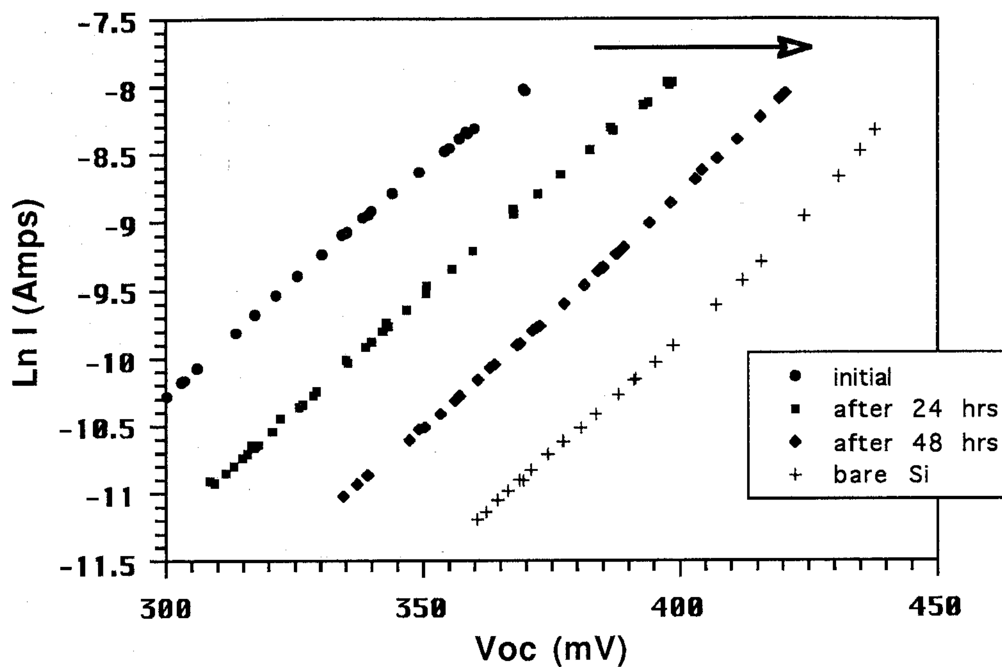

Figure 8: Plot showing I-V data gathered on the same silicon electrode (patterned with 100 nm-wide metal lines, in $Me_2Fc^{+/0}$-methanol solution) on three successive days. In between each measurement, the electrode was left in air for ~24 hours, and was etched in HF immediately before immersion into solution.

Stability of Silicon/Gold Junctions

As can be seen in figure 8, there were some problems with the stability of the gold/silicon contacts of the electrodes patterned with 100 nm-wide gold lines. During the electrochemical measurements in solution, a shift in the current-voltage properties of the same electrode was observed over several succesive measurements; between each measurement, the electrode was left in air, and then re-etched in the buffered HF solution before being placed back into the electrochemical solution cell. This shift, towards higher photovoltages at similar photocurrent, can be interpreted as a decrease in the effective metal/silicon contact area. SEM of this electrode (figure 9) revealed numerous areas where the gold adhesion to the silicon had failed, and the metal lines had become detached from the surface.

One explanation may be that in air, a thin layer of silicon on the surface could have oxidized. This oxide growth could have undercut the edges of the metal lines. Removal of the oxide layer by etching in HF would leave the edges of the metal no longer in contact with the silicon. Repetition of this process would reach further underneath the gold lines and would result in the metal completely losing contact with the silicon, and the metal lines would become detached from the surface. The shift in the current-voltage characteristics that occurs with the electrodes is not seen for the electrodes with 5 μm-wide lines over analogous time periods and etching procedures, possibly because the amount of undercutting at the edge of the metal line relative to the width of the metal line is quite small.

An interesting feature in figure 9 is that a "shadow" image of the original metal lines is evident on the silicon surface where the metal lines have become detached. It is unknown if this is indicative of metal-silicide formation, or if it is merely that the silicon beneath the metal lines is at a slightly different height from the surrounding areas.

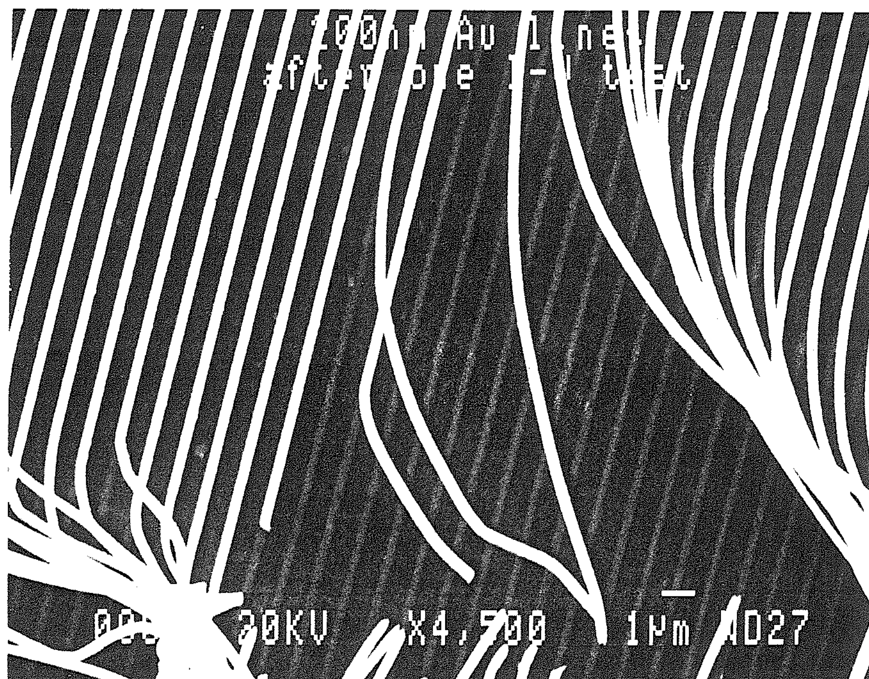

Figure 9: SEM showing the partial removal of 100 nm-wide gold lines from the silicon surface during electrochemical measurements in $Me_2Fc^{+/0}$-methanol solution. After several experiments, the gold was easily removed from the entire surface by using Scotch Tape. Note the faint line patterns remaining on the silicon underneath the detached gold lines. This problem did not occur with platinum.

Part 3: Modification of Electrode Design

One of the main reasons for using the metal-line patterns in this study was that the area of metal/silicon contact would be accurately known. However, this knowledge is less useful if it cannot be determined that all of the metal makes a good junction with the silicon. The fact that there is a shift in the solution current-voltage properties of the electrode with 100 nm-wide gold lines is evidence that there is initially electrical contact between the metal and the silicon. It is difficult to determine, however, if the initial electrical junction area between the gold and the silicon is equal to the measured area of the metal lines. The initial set of data could represent an already partially degraded connection, and subsequent data sets merely track the worsening connection. It became evident after this experiment that an alternative method of determining the extent of the silicon/metal contact would be needed. We developed several methods which could be used to measure the true area of Schottky junction formation on a given electrode.

The first method attempted was simply to solder a wire to a small piece of a razor blade, and lower this to the surface of the electrode in an attempt to contact all of the metal lines. In this way, I-V measurements of the metal/ silicon junction could be made and compared with the expected results based on the measured metal area. Thus, any difference in the data collected in this manner as compared to the data collected in the solution cell would be evidence of a shielding effect on the metal areas by the solution depletion region. However, the razor proved to be very rough on the metal lines, and

often scraped up large areas of the pattern. In addition, there was again no way to determine if all of the lines were actually being contacted (eg. any notch in the razor would fail to contact the underlying line).

The second method attempted is depicted in Figure 10. First, two insulating silicon oxide layers were grown on the silicon surface, and a metal contact pad was deposited on top of these oxide layers. Then, metal lines were deposited onto the silicon in the same manner as previously described such that they overlapped the metal contact pads. The metal lines running left to right in Figure 10 were to be simultaneously in contact with the silicon and the two metal contact pads on either side. These contact pads would not in any way affect the current-voltage properties of the device, because they are insulated from the silicon by the oxide layer.

This device design would allow all of the current coming through the front of the electrode to be collected directly from the contact pads for measurements done in air. In addition, current could still be measured while the electrode is in solution. Thus, in solution, if the metal areas become shielded from the semiconductor by the solution depletion region, the current-voltage properties of this electrode should be different from those measured in air.

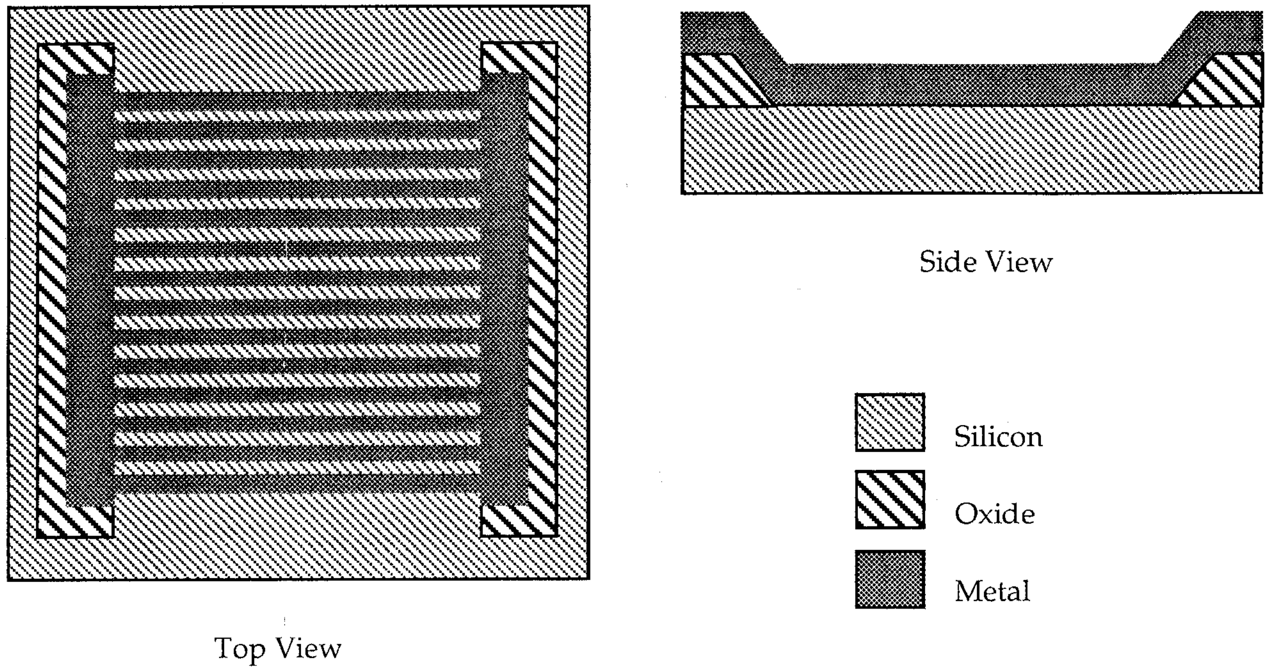

Figure 10: Schematic of a design that would allow measurement of current through the metal-silicon junction directly, as well as the junction formed in solution. Various difficulties encountered in the fabrication process prevented the device from successfully being made.

This design, however, incorporated several additional difficult fabrication steps. The metal contact pads on the sides of the metal line pattern had to be deposited in a separate step; platinum and gold have very poor adhesion to silicon oxide, and a chromium/gold or titanium/platinum bilayer was required for this step. Then, the standard fabrication procedure for the metal line pattern was followed. However, due to undercutting of the oxide layer during the HF etching step, no connection was made between the lines and the contact pads. At this time, this design was determined to be too difficult to fabricate.

A slight modification of the original electrode design was attempted, involving a similar concept. One thicker metal bar (e.g. 10 μm wide) was deposited across the array of metal lines such that the thicker cross-bar was in contact with all of the other lines (figure 11). The lines were all deposited in the same metal evaporation step, thus avoiding the possible problems of poor adhesion and electrical contact between different layers of metal. By contacting this thicker line and using it to collect current for measurements of silicon/metal junction properties made out of solution, a similar comparison of solution vs. non-solution current-voltage characteristics was made. The 10 μm wide crossbar made less than a 1% contribution to the overall metal area.

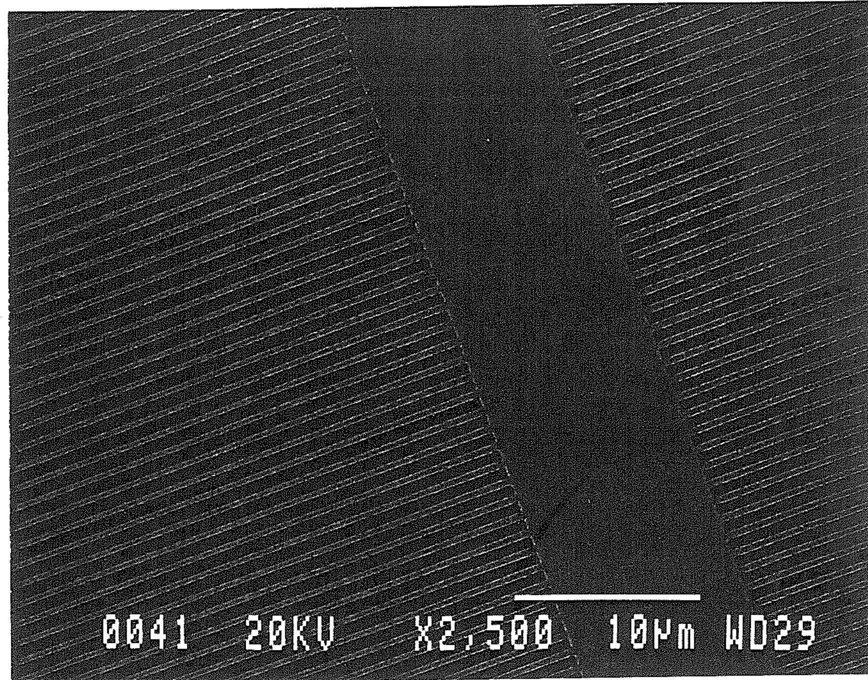

Figure 11: SEM of redesigned metal-line pattern, showing the 10 µm-wide line perpendicular to the ~340 nm-wide lines and used as a contact for collecting current. The net area increase cause by the contact line is less than 1% of the total metal area, and therefore has only a small contribution to the net current-voltage properties of the electrode. The 340 nm-wide lines are somewhat wider in the vicinity of the 10 µm-wide line due to the scattering of the electron-beam at the higher current level used to write the cross-line.

Part 4: I-V Characteristics of Silicon/Platinum Junctions

The decision to use platinum instead of gold was arrived at for several reasons. Platinum was found to have better adhesion properties than gold, and unlike gold, platinum had a long-term stability in regard to the electric junctions formed with silicon. Several weeks after fabrication of the platinum devices, the current-voltage properties remained unchanged, while those for the gold devices changed markedly. In addition, several of the previous studies involving discontinuous films and small particles deposited on the surface of silicon had been done using platinum[5-9]. Thus, using platinum for the lines seemed a more direct study of the mechanisms in these systems.

The solution I-V properties of the electrodes with 5 µm-wide platinum lines were found to depend on metal coverage in a similar manner to the electrodes patterned with 5 µm wide gold lines, i.e. a larger percentage of metal coverage elicited a smaller V_{oc} at a given photocurrent level. The electrodes with 5 µm-wide platinum lines were fabricated with 10 or 20 µm crossbars, which were contacted in air with a platinum wire to measure the silicon/metal electrical junction properties. It was found that contacting the crossbar at several different spots on any given electrode gave similar I-V measurements, indicating that this was an effective method for determining the extent of formation of the silicon/platinum junction.

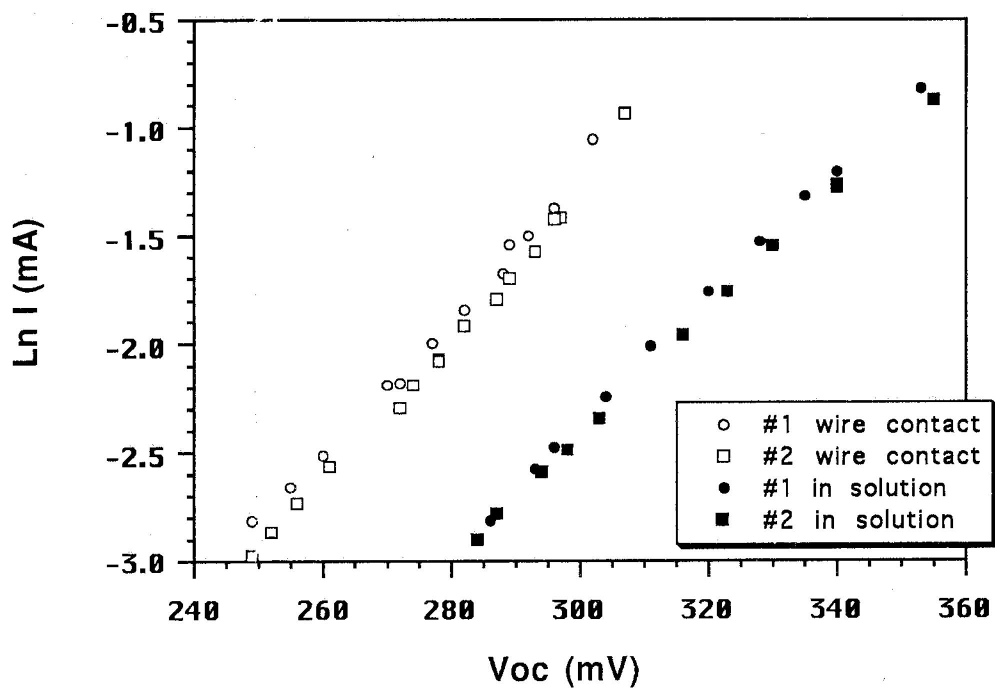

Figure 12: I-V properties of two separate silicon electrodes patterned with 5 μm-wide platinum lines, both in $Me_2Fc^{+/0}$-methanol solution and in air (measured by platinum wire contacts to the cross-lines). The closed data symbols are for measurements for each electrode made in solution; the open symbols are for measurements made in air.

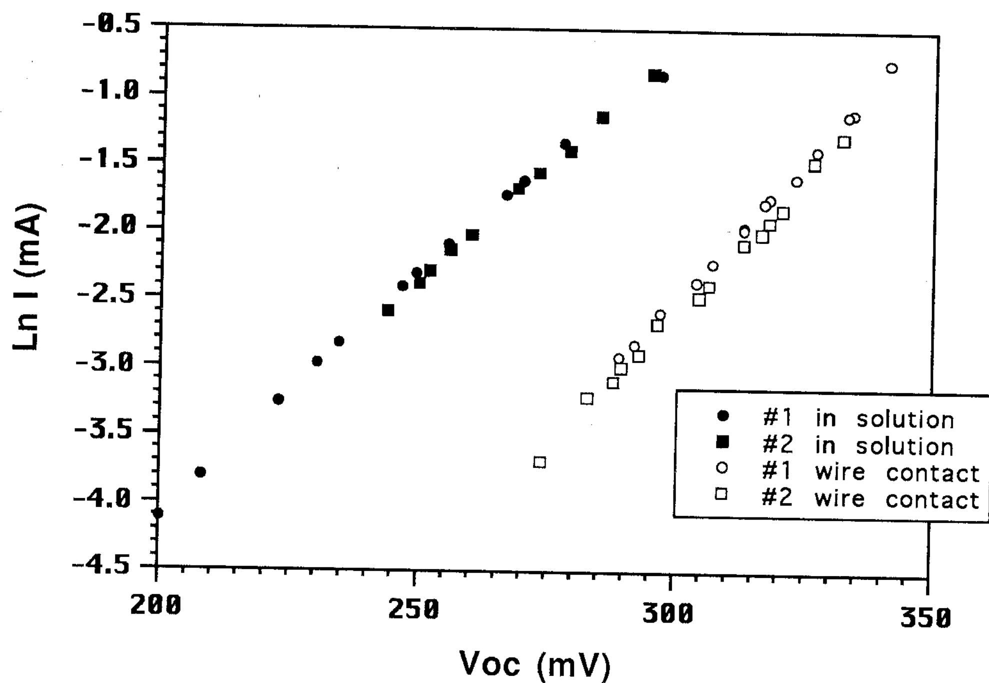

Figure 13: I-V properties of two separate silicon electrodes patterned with 340 nm-wide platinum lines, both in $Me_2Fc^{+/0}$-methanol solution and in air (measured by platinum wire contacts to the cross-lines). The closed data symbols are for measurements for each electrode made in solution; the open symbols are for measurements made in air.

A comparison of the data for the electrodes patterned with 5 μm-wide platinum lines is shown in figure 12. Current-voltage measurements made in air exhibit V_{oc} and I_0 values that are expected for a silicon/platinum Schottky junction (represented on the graph by the open symbols). Measuring the current-voltage properties of the same electrode in solution (represented by the closed symbols) showed a shift towards lower current at a given V_{oc}, possibly meaning that even for this system the metal lines are partially shielded by the undercutting of the solution depletion region. However, the I_0 values determined for the electrodes patterned with 5 μm-wide platinum lines in solution are again the expected values for a silicon/platinum Schottky junction.

The examination of silicon electrodes patterned with sub-micron-wide platinum lines resulted in data that are difficult to interpret. When these electrodes were placed into solution, they exhibited lower photovoltages for similar current levels relative to the results obtained for the electrodes with 5 μm-wide platinum lines. However, the I_0 values determined for the electrodes with sub-micron-wide platinum lines is very similar to the values obtained for the electrodes with 5 μm-wide platinum lines. In other words, in solution the electrodes' current-voltage behavior appeared to be independent of line width.

The current-voltage properties of the electrodes with sub-micron-wide platinum lines were also examined out of solution, using the same platinum-

wire front contact. These electrodes exhibited larger V_{oc} values out of solution (figure 13); however, the I_0 values measured in air were two orders of magnitude smaller than expected for a silicon/platinum Schottky junction, based on the area of metal coverage.

Conclusion

Based on these results, it is difficult to determine what processes are taking place near the surface of these metal-line coated electrodes. Using gold lines resulted in data that seemed to validate the theory; however, the inability of gold to form a long-term, stable contact with silicon raises doubts as to the interpretation of this data. The electrodes with sub-micron-wide platinum lines exhibited almost no difference in current-voltage properties relative to the electrodes with the larger width platinum lines. The I_0 values found for the electrodes with 5 μm-wide platinum lines, both in air and in solution, were as expected for a typical silicon/platinum Schottky junction. The electrodes with the sub-micron-wide platinum lines also exhibited these expected values in solution; as measured in air, however, they showed a much lower I_0 value than expected. This result seemed to contradict not only the theory, but also the results obtained for the electrodes with gold lines. However, the differences in results could easily be attributed to incomplete current collection from the front contact. If only a fraction of the current was collected from the silicon/platinum junction in air, it would appear to have a much lower current than would be expected based on the metal/silicon junction area.

Future work should focus on the difficulty in measuring the current-voltage properties of these electrodes outside of solution, i.e. determining the area of the metal/silicon junction. A clear, accurate and reproducible method for measuring this data would allow the differentiation to be made between

faulty current-voltage measurements and data which reinforces the proposed theory. One other possible method of doing this, besides those mentioned in this thesis, would be to passivate the silicon surface of the electrode, preferably by reversibly binding some compound to the surface that will electrically insulate the silicon from the solution. The current-voltage properties of the metal/silicon junction can then be measured in solution, using the solution as the front contact for the metal lines.

Future work could also follow the route of using p-type silicon instead of n-type. It has been shown that p-type silicon forms ohmic contacts with metals, but is rectifying in solution[2]. This way, instead of attempting to measure a shift in current-voltage properties between two rectifying systems, a more definite difference would be produced, that of rectifying compared to ohmic.

References

(1) Tan, M.X.; Laibinis, P.E.; Nguyen, S.T.; Kesselman, J.M; Stanton, C.E.; Lewis, N.S. *Progress in Inorganic Chemistry*, **1994**, *41*.

(2) Lewis, N.S. *Accounts of Chemical Research*, **1990**, *23*, 176-183.

(3) Sze, S.M. *Physics of Semiconductor Devices*, 2nd ed.; J. Wiley: New York, 1981.

(4) Tan, M. *Ph.D. Candidacy Report*, Caltech, 1991.

(5) Nakato, Y.; Ohnishi, T.; Tsubomura, H. *Chem. Lett.* , **1975**, 883-886.

(6) Allongue, P.; Souteyrand, E.; Allemand, L. *J. Electrochem. Soc.* **1989**, *136*, 1027-1033.

(7) Ueda, K.; Nakato, Y.; Suzuki, N.; Tsubomura, H. *J. Electrochem. Soc.* **1989**, *136*, 2280-2285.

(8) Nakato, Y.; Yano, H.; Tsubomura, H. *Chem. Lett.* **1986**, 987-990.

(9) Nakato, Y.; Ueda, K.; Yano, Y.; Tsubomura, H. *J. Phys. Chem.* **1988**, *92*, 2316-2324.

(10) Elliot, D.J. *Integrated Circuit Fabrication Technology*, 2nd. Ed., McGraw-Hill, 1989, 97-99.

(11) Brewer, G. (Ed.) *Electron-Beam Technology in Microelectronic Fabrication*, Academic Press, 1980, 11-26.

(12) Muller, R., personal communication.